

Causality detection and turbulence in fusion plasmas

B.Ph. van Milligen¹, G. Birkenmeier², M. Ramisch³, T. Estrada¹, C. Hidalgo¹, A. Alonso¹

¹Laboratorio Nacional de Fusión, Avda. Complutense 40, 28040 Madrid, Spain

²Max Planck Institute for Plasma Physics, Boltzmannstr. 2, 85748 Garching, Germany

³Institut für Grenzflächenverfahrenstechnik und Plasmatechnologie, University of Stuttgart, 70569 Stuttgart, Germany

The problem of determining the causal relationship between various interacting fields or variables is of fundamental importance in many branches of science. Knowledge of the causal connection between variables is helpful for the elaboration of a realistic physical model and/or to check its validity. Causality is notoriously hard to define in general [1]. In the present work, we do not use the term ‘causality’ in its philosophical, absolute sense (if Y occurs, then X will occur; or: if X occurs, then Y must have occurred). Rather, we turn to the concept of ‘quantifiable causality’ introduced by Wiener [2] (rephrased slightly): *For two simultaneously measured signals X and Y , if we can predict X better by using the past information from Y than without it, then we call Y causal to X .* Different methods have been proposed to evaluate this property [1]; here we will use a non-parametric procedure for causality detection originating in the field of information theory: the ‘Transfer Entropy’ [3].

Method

Consider two processes X and Y yielding discretely sampled time series data x and y . A measure of information transfer between the two time series X and Y is given by the *Transfer Entropy* [3]:

$$T_{Y \rightarrow X} = \sum p(x_{n+1}, x_n^{(k)}, y_n^{(l)}) \log_2 \frac{p(x_{n+1} | x_n^{(k)}, y_n^{(l)})}{p(x_{n+1} | x_n^{(k)})} \quad (1)$$

where $x_n^{(k)}$ indicates a set of k data values of the time series x preceding or coinciding with the time associated with time index n , and p indicates a probability density. $T_{Y \rightarrow X}$ measures the excess amount of bits needed to encode the information of the process X at time point $n + 1$ with respect to the assumption that this information is independent from Y . Thus, the Transfer Entropy is an implementation of Wiener’s ‘quantifiable causality’. If Y has no influence on the immediate future evolution of system X , one has $p(x_{n+1} | x_n^{(k)}, y_n^{(l)}) = p(x_{n+1} | x_n^{(k)})$, so that $T_{Y \rightarrow X} = 0$. $T_{Y \rightarrow X}$ can be compared to $T_{X \rightarrow Y}$ to uncover a net information flow.

The probability distributions appearing in Eq. (1) are calculated using a discrete binning of m bins in each coordinate direction. The main joint pdf $p(x_{n+1}, x_n^{(k)}, y_n^{(l)})$ has $l + k + 1$ dimensions, so there are m^{l+k+1} bins, and this number should be much smaller than the available length

of the data arrays, N , in order to obtain a statistically significant sampling of the pdf. For this reason, we will set $l = k = 1$ and $m = 3$ in the following.

TJ-K

The TJ-K stellarator is a torsatron operated at low magnetic field ($B = 72$ mT) and low plasma beta. The discharge analyzed here corresponds to a helium plasma, heated by microwaves, with a central density of $n = 2.3 \cdot 10^{17} \text{ m}^{-3}$ and an electron temperature of $T_e = 8$ eV and cold ions, as reported in more detail elsewhere [4]. In this experiment, turbulence was dominated by electrostatic drift wave turbulence, and the total particle transport and zonal potential were found to be linked in a predator-prey cycle. We use data from a set of 64 Langmuir probes, distributed over a poloidal circumference of the device. We compute the zonal potential $\Phi_z(t)$ as the mean poloidal value of the floating potential, and the global radial particle flux $\Gamma_{\text{tot}}(t)$ as the poloidal mean of the local radial particle flux.

Fig. 1 shows the Transfer Entropy between the two signals $\Phi_z(t)$ and $\Gamma_{\text{tot}}(t)$ as a function of the lag $l = \alpha$ and $k = \beta$. The amplitude of the Transfer Entropy is rather small, namely below $5 \cdot 10^{-3}$, compared to the full bit range $\log_2 m = 1.59$, which indicates that the causal link between these variables is not very strong. Nevertheless, it is unexpected and interesting to observe that $T_{\Phi \rightarrow \Gamma}$ and $T_{\Gamma \rightarrow \Phi}$ peak at different values of $\alpha = \beta$. Thus, zonal potential Φ_z has a rather fast impact on the total particle flux Γ_{tot} , while the total particle flux Γ_{tot} acts back on the zonal potential Φ_z on a much longer time scale. The short time scale result confirms the analysis of [4]. The long time scale result is presumably due to a restoration of ambipolarity: a modification of transport must eventually lead to a modification of potential.

TJ-II

TJ-II is a Heliac type stellarator with 4 field periods. The experiments discussed below have been carried out in pure Neutral Beam Injection (NBI) heated plasmas (line averaged electron density $\langle n_e \rangle = 2 - 4 \times 10^{19} \text{ m}^{-3}$, central electron temperature $T_e = 300 - 400$ eV, $T_i \simeq 140$ eV).

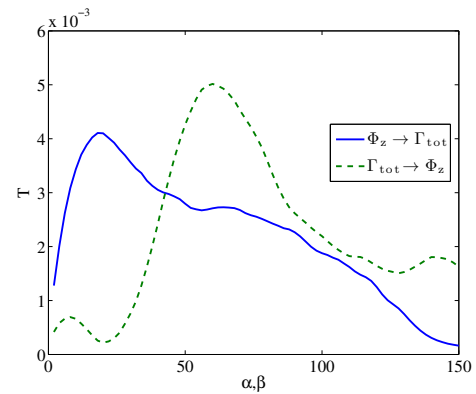


Figure 1: Transfer Entropy between the zonal potential $\Phi_z(t)$ and the global particle transport $\Gamma_{\text{tot}}(t)$ at TJ-K versus $\alpha = \beta$ (in sampling units, i.e., μs).

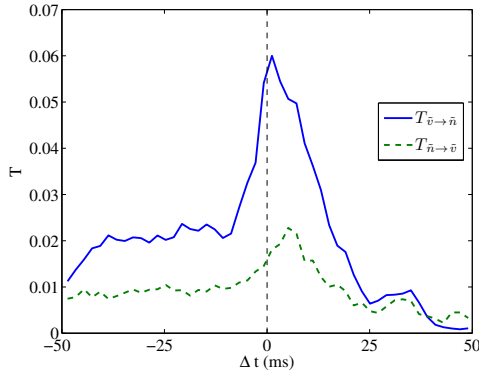


Figure 2: Mean Transfer Entropy between \tilde{v}_\perp (the fluctuating perpendicular flow velocity) and \tilde{n} (the turbulence amplitude) for 10 discharges in a magnetic configuration with $\iota(a)/2\pi = 1.553$ (the L-I transition occurs at $\Delta t = 0$).

The Transfer Entropy $T_{\tilde{v}_\perp \rightarrow \tilde{n}}$ increases sharply by a factor of 2 at the L–H transition, indicating the regulation of turbulence (\tilde{n}) by the Zonal Flow (\tilde{v}). This regulatory phase lasts for about 15 – 20 ms, in accord with the duration of enhanced bicoherence reported elsewhere [6].

We draw attention to an interesting difference between the L–I and L–H transitions. With the L–H transition, the transition is followed by a rapid increase in $T_{\tilde{v}_\perp \rightarrow \tilde{n}}$, while $T_{\tilde{n} \rightarrow \tilde{v}}$ remains approximately constant. Thus, the Zonal Flow is simply regulating the turbulence (suppressing it). With the L–I transition, the transition also shows a rapid increase of $T_{\tilde{v}_\perp \rightarrow \tilde{n}}$, but this is mirrored (although at a lower intensity level) by a similar increase in $T_{\tilde{n} \rightarrow \tilde{v}}$. This is

consistent with the fact that not only does the Zonal Flow regulate the turbulence, but the turbulence also acts back on the Zonal Flow, which could be related to the observed (predator-prey

The input NBI power was about 500 kW. We analyze data from the Doppler reflectometry diagnostic taken as the plasma experiences spontaneous confinement transitions [5]. The Doppler reflectometer signals, sampled at 10 MHz, allow determining \tilde{n} and v_\perp with high temporal resolution.

Fig. 2 shows the mean evolution of the Transfer Entropy for 10 discharges in a magnetic configuration with edge rotational transform $\iota(a)/2\pi = 1.553$. In this configuration, a transition from L-mode to an Intermediate (I) phase is often observed (intermediate between the L and H modes).

Next, we consider discharges in a magnetic configuration with $\iota(a)/2\pi = 1.630$. In this configuration, a relatively rapid transition from L-mode to H-mode is often observed, without intermediate (I) phase [5]. Fig. 3 shows the average evolution of the Transfer Entropy for 4 discharges in this magnetic configuration (around the L–H transition).

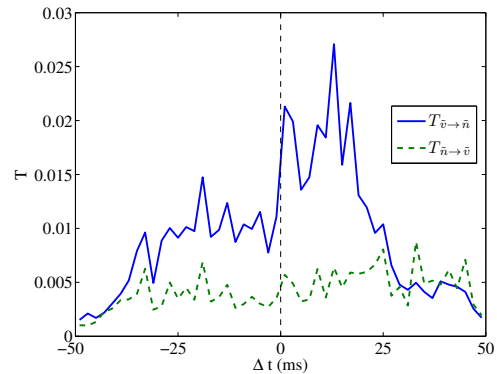


Figure 3: Mean Transfer Entropy between \tilde{v}_\perp (the fluctuating perpendicular flow velocity) and \tilde{n} (the turbulence amplitude) for 4 discharges in a magnetic configuration with $\iota(a)/2\pi = 1.630$ (the L–H transition occurs at $\Delta t = 0$).

type) oscillations. Also, in the case of the L–I transition, the values achieved by the Transfer Entropy are about 3 times higher than with the L–H transition. In both cases, the amplitude of the Transfer Entropy is modest compared to the bit range, $\log_2 m = 1.59$, although an order of magnitude above the TJ-K case reported in the preceding section.

Conclusions

We have explored the application of the Transfer Entropy technique to some data from turbulent fusion plasmas, clarifying the interaction between the Zonal Flow and turbulence. The analysis of the global potential and flux at TJ-K revealed the existence of two time scales: 20 and 60 μs . Doppler reflectometry data from TJ-II taken across L–I and L–H transitions in NBI heated plasmas showed how the fluctuating perpendicular flow velocity \tilde{v} , again associated with Zonal Flows, affects the turbulence.

Comparing the TJ-K and TJ-II results, we note that the amplitude of the Transfer Entropy is about an order of magnitude higher in the latter device. Presumably, this corresponds to a larger Zonal Flow amplitude generated by a stronger drive (steeper gradients). From the numerical and experimental examples examined in this work, it is concluded that the Transfer Entropy constitutes a powerful tool to unravel the causal relationship between nonlinearly interacting fields in complex systems. It is expected that this technique may find applications in many fields of research.

Research sponsored in part by the Ministerio de Economía y Competitividad of Spain under project Nr. ENE2012-30832.

References

- [1] K. Hlaváčková-Schindler, M. Paluš, M. Vejmelka, and J. Bhattacharya. *Phys. Reports*, 441(1):1, 2007.
- [2] N. Wiener. *The theory of prediction*. Modern Mathematics for Engineers. Mc-Graw Hill, New York, 1956.
- [3] T. Schreiber. *Phys. Rev. Lett.*, 85(2):461, 2000.
- [4] G. Birkenmeier, B. Ramisch, M. ans Schmid, and U. Stroth. *Phys. Rev. Lett.*, 110:145004, 2013.
- [5] T. Happel, T. Estrada, E. Blanco, C. Hidalgo, G.D. Conway, U. Stroth, and the TJ-II Team. *Phys. Plasmas*, 18:102302, 2011.
- [6] B.Ph. van Milligen, T. Estrada, C. Hidalgo, T. Happel, and E. Ascasíbar. *Nucl. Fusion*, 53:113034, 2013.